Investigating the Reliability of Existing TA-SP Semi-rigid Connection System by Advanced Modeling Techniques

Ferid A. Yonis [*] , Chun-Qing Li , Saman De Saliva [*]

Article

Investigating the Reliability of Existing TA-SP Semi-rigid Connection System by Advanced Modeling Techniques

Ferid A. Yonis [1,*], Chun-Qing Li [2] and Saman De Saliva [3,*]

1   Structural and Civil Engineer, RMIT University, Melbourne VIC 3000, Australia
2   STEM College, School of Engineering, RMIT University, Melbourne VIC 3000, Australia
*   Correspondence: fayonis@yahoo.com.au (F.A.Y.); saman.desilva@rmit.edu.au (S.D.S.)

Abstract: This investigation introduces an efficient method for assessing the reliability of semi-rigid steel frame connections in existing buildings, explicitly targeting the Top Angle and Seat Pad (TA-SP) semi-rigid connection commonly used in Australian cities' high-rise buildings. The ultimate capacity of these connections was examined through parameter power model testing, considering the bending, shear, and prying forces actions to determine the weakest elements in the system. A plastic hinge model was applied to ensure computational efficiency and accuracy in assessing the connections' ultimate strength. Comparatively, the finite element (F.E) method $M-\theta$ curves were introduced to examine the nonlinear behaviour of the connection, providing validation for the predicted analytical approach. Further emphasis was placed on identifying the reliability of the weakest elements in the connection system, employing the First-Order and Second-Order Reliability Methods models to estimate their reliability index. The correlation between the model's failure probability and a percentile error was also explored, utilising Monte Carlo simulation reference for refined validation. Novel formulas and methodologies were introduced to compute the locked-chain-series system reliability, which accounts for the inherent material and geometric variability. The findings highlight the critical significance of the weakest element in determining the overall reliability of the existing TA-SP connection.

Keywords: semi-rigid connection; $M-\theta$ relationship; finite element F.E.; locked chain series system; reliability index; system reliability index; target reliability index

1. Introduction

The interest is increasing in developing assessment methods or possibilities for determining the reliability of the existing ageing building's frames. Notably, the ageing building's frames exposed to lateral force were a significant hazard source and the primary requirement of a safety measure. Therefore, many recent studies have focused on evaluating building resilience, i.e., the holistic ability to minimise loss through reliability, redundancy, and recoverability against extreme loads. Indeed, considering uncertainties in seismic demands, the response values of existing building members, such as beams, columns, and connections, exhibit significant correlations due to uncertain ground motion strengths.

However, assessing the seismic safety of older aging buildings that do not meet current design standards necessitates a fast and effective method. In this context, gathering all available data, including construction materials and structural drawings, is crucial to understanding the interconnected members of the building and the flexibility of its structural system. In this case, many numerical models were developed to assess the connection flexibility, offering valuable insights into the underlying system. Hardy Cross [1] is accredited for his contributions to understanding structural behaviours, especially the rotational flexibility of connections. Since then, considerable experimental and numerical work has been carried out, leading to the development of the semi-rigid connection.

In the early design development stage, riveted, bolted, and welded connections contributed to how the semi-rigid connections transmit forces and deform under various load conditions. This

information is now well-established and integral to the design methods. The design codes, such as AISC-LRFD [2] and Eurocode 3 [3], provide deep insight into the design model that considers the moment-rotation relationships. The applications of design model parameters, such as initial stiffness (Rki), ultimate moment capacity (Mu), and shape parameter (n), are essential factors in semi-rigid connections. The backgrounds of detailed experimental tests and numerical analysis are vigorously accessible in the preceding works of literature – see, for example, Richard and Abbott [4] Kishi and Chen [5], Colson and Louveau [6], Azizinamini et al. [7], Bjorhovde Colson & Brozzetti [8], Pekcan, Mander and Chen [9], Faella et al. [10] and Ahmed et al. [11]. The review regarding the established methodologies is clearly outlined in (ANSI/AISC 360-10 and Eurocode 3 Part 1- 8) [3]) which permit the consideration of the semi-rigid behaviours that reflect the ranking in the classification.

Over the past few decades, designing a semi-rigid connection has been challenging due to the complex calculations required to determine the influential parameters factor. Therefore, extensive research has been carried out to develop advanced analysis techniques that accurately account for the parameters' power mode of the semi-rigid connections using the three-dimensional nonlinear finite element analysis. The 3D version is a virtual reality that uses advanced computer modelling technology to enhance design concepts. The work of Pirmoz & Danesh [12] and Smitha & Babu [13] provides early insight into the need to consider the moment-rotation behaviour on bolted top and seat angle connections using the F.E. method. Ahmed et al. [14] developed a nonlinear finite element model to investigate the effects of prying forces thoroughly and involved rigorous analysis of the moment-rotation behaviour of T-SA connection with double web angles. The results indicated that the local contact area influences the connection parameter profiles. Further, Diaz et al. [15] comprehensively reviewed more literature and outlined the significant findings of various semi-rigid connections.

The main focus of this paper is to assess the reliability of the existing Top Angle and Seat Pad (TA-SP) connection, widely utilised in high-rise buildings across Australian cities erected from the 1920s to the 1960s. The semi-rigid connection types within the building frame joints combine stiffness and flexibility, presenting a unique characteristic compared to entirely rigid or flexible connections. This specific connection has not been previously studied, and no established procedures exist to analyse its behaviour. The connection system consists of various elements exposed to tensile force, and the weakest elements can be susceptible to bending-type behaviour. The tensile strength at which bending occurs is the design criterion for the compression of the elements.

Meanwhile, a computer program model is a convenient method to assess the F.E. nonlinear behaviours of an existing connection, enabling the characterisation of failure behaviours while ensuring both safety and operational efficiency. The structural reliability methods model also provides a standardised method to assess the overall connection system reliability at multiple levels. In this context, the current study focuses on analysing changes in the cross-section of the weakest elements to evaluate the system reliability of existing connections.

Both approaches mimic a fast seismic advancement gaining significance due to the widespread use of the TA-SP connection in Australian metropolises. Moreover, the basic principle of the structural reliability concept may pose challenges, as it involves assessing the failure probability of the weakest elements. This evaluation is intricately linked to the overall cross-section of the existing connection, magnifying the probability of system failure. Hence, the system reliability index becomes the foundation of a new method that aligns with the essential criteria of ISO 13822 [16], ISO 2394 [17], and JCSS [18].

2. Investigation Methods and Framework

The primary purpose of the current study is to estimate the reliability of the existing TA-SP semi-rigid connection. For this reason, a comparison was conducted between the existing connection's theoretical representation and the nonlinear finite element (F.E.) analysis method using ABOUCS [19] computer programs.

However, the general results cannot be dependable measurement sources, as the uncertainties cause significant errors. Therefore, it is imperative to exercise carefulness and not be considered based

solely on the results of any critical decisions. For instance, loading, material properties, and engineering models are primary measures of uncertainties.

Hence, structural reliability methods that refer to an organised investigation approach were proposed for the current research and investigation purposes. This delineates various reliable methods for efficiently gathering and organising information that is applicable across computational models. This includes the First Order Reliability Method (FORM) [20] and the Second Order Reliability Method (SORM) [21], which were initially introduced. This is followed by the Monte Carlo simulation (MCS) [22], which plays a vital role in validating the accuracy of the analysis, particularly in determining the failure probability of the existing connection.

In this context, the steps are essential in capturing the essence of the new approach initiating a system reliability study. Therefore, the following inclusive flowchart outlines the steps in Figure 1 to streamline the process and address the existing connection reliability issues.
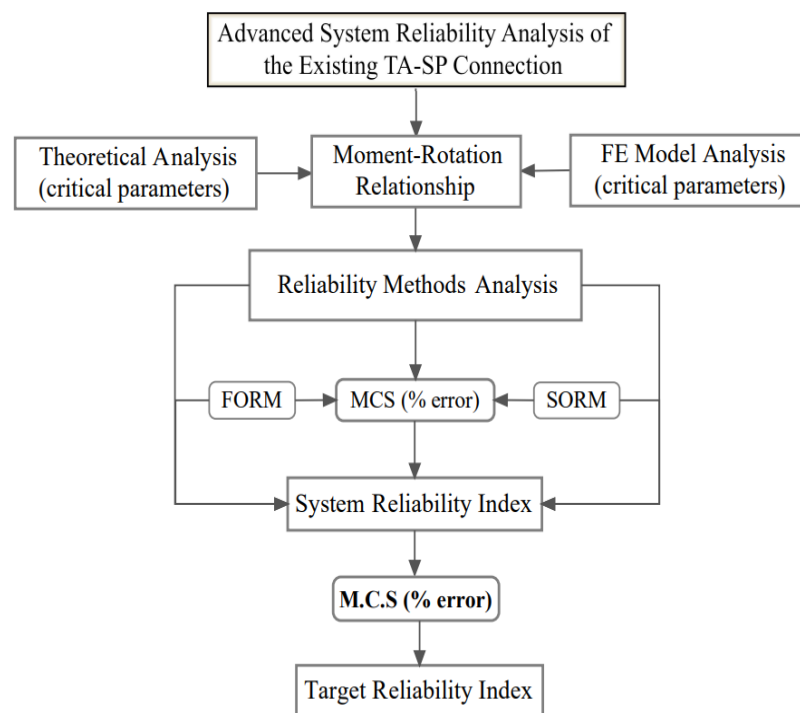

Figure 1. Flowchart for the proposed investigation methods.

2. Deterministic Analyses of the Existing Connection System

2.1. Assessing the Failure Probability in the TA-SP Connection System

The prototype of the TA-SP connection model is proposed to determine the reliability index and the probability of failure. Typically, failures involve multiple random variables related to the connection system, expressed through the system's failure modes. The model shows a sequence of interconnected elements; accordingly, despite the complexity of the connection system, Figure 2 depicts the existing TA-SP connection prototype containing ten independent elements.
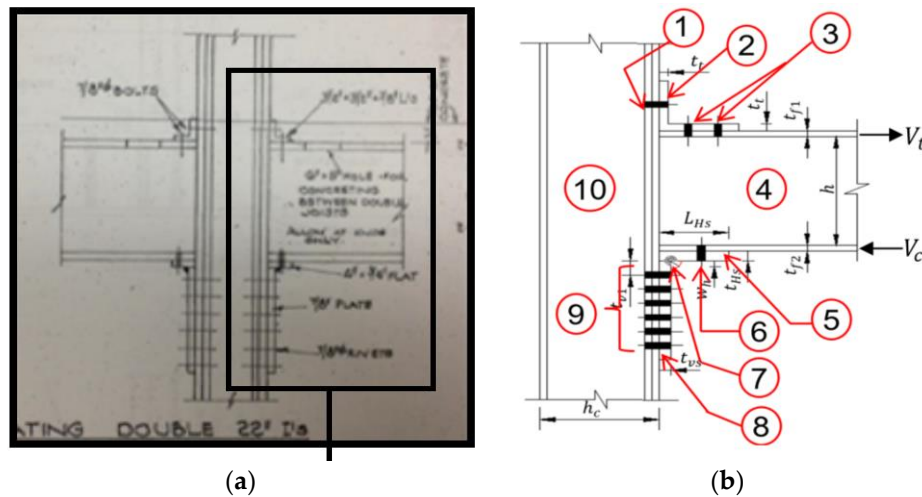
Figure 2. Existing TA-SP semi-rigid connection prototype: (**a**) represents a typical 1920- 1960s semi-rigid connection used in Australian metropoles and (**b**) describes the TA-SP connection elements.

However, it is crucial to note that the existing connection model operates within a statically determined framework, rendering it susceptible to system failures. This vulnerability stems from the possibility of plastic hinges forming in any of its weakest elements. Consequently, such hinge development can trigger failures across the connection system. Intrinsically, each element of the model is susceptible to failure mode and therefore, the probability of the system failure is based on the weakest link of the *n-th* element, as previously quoted by the expression of Freudenthal [23]

$$P_f \approx P(E_1 \cup E_2 \dots \dots \dots \dots \cup E_n), \tag{1}$$

Where E_i= the event failure in an i-th mode of $(i = 1,2,3 \dots n)$. Hence, the probability of system failure can be expressed by:

$$P_f \approx P[\text{g}(X) \leq 0] \approx \int \dots \int f_x(x) \, \partial_x, \tag{3}$$

Where $f_x(x)$, is the joint probability of the density function of stochastic variables, and the g(X) = 0 is the limit state function, Where X is a vector of stochastic variables of the system and can be defined using the relationship between the applied force X_{Fi}, and the resistance of the element X_{Ri}, where X is $(x_1 \dots x_n)$ of the system variables, and n is a physical model of statistical uncertainty. In this context, the limit state event is merely expressed by the conditions of g(X) $\geq$ 0 is safe and relatively g(X) < 0 is failure set, and the relevant equation can then be described as:

$$\text{g}(X) \approx F(X_{Ri}) - F(X_{Fi}), \tag{3}$$

Where F_i, is a function of shear force in *i-th* element, and R_i is the resistance of the *i-th* element. With such a perspective, the expression of Weibull gives the cumulative distribution function of the *i-th* strength, as given in the following equation [24]:

$$F_{Ri}(r) \approx 1 - \prod_{i=1}^{m} [\, 1 - F_{Rn}(r_n)], \tag{4}$$

2.2. Analysing the TA-SP Connection Through Locked Chain System

The semi-rigid connection consists of unified inter-reliant mechanisms. Its performance is governed by the limit state function and is assumed to have two crucial conditions: the system's functional and failure state. System failure is then related to the individual element, and the forces can be either in the state of function or failure. For instance, if one of the elements fails, the other elements may not hold the connection system and instantaneously cause a brittle failure with low statical determinations. This type of failure is expressed by the failure mode of the individual component *En* and is likely to lead to a series of system failures. For instance, Figure 3 illustrates that

the locked chain-series system comprises ten independent elements of the existing connection, which expresses their applications to the failure modes.
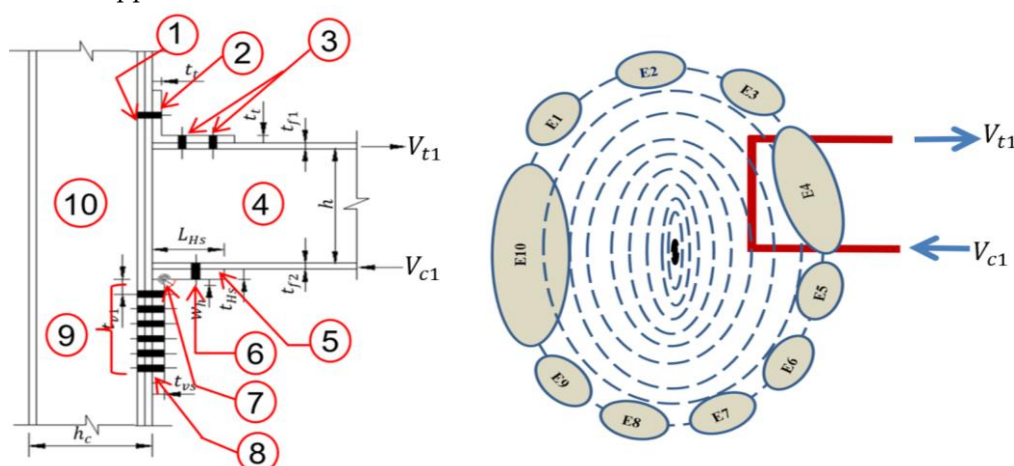

Figure 3. Locked chain-series system of the existing TA-SP connection.

Generally, failure can occur through the applied tensile forces on the system performance, and Xi represents the force distribution among the elements. Relatively, the strength of the connected elements distribution is denoted by Si. Where (*i*) is the failure event of the *i-th* element and *i* = 1, 2, ... *n*. Thus, the failure state of the weakest link element is given by En = {Xi > Si}, and the domain conditions are the clockwise rotational failure mechanism of the connection signifying the failure event. Accordingly, the failure probability of the union events from the limit state function is given by rearranging Equation 1.

$$P_f \approx \sum_{n=1}^{i=n} P_{f1} \cup P_{f2} \ldots \cup P_{fn}. \tag{5}$$

In this instance, the applied force and resistance are stochastic variables. Past experimental test data likely define the resistance parameters of the existing connection elements. The integral functions of the parameters represent a mean and standard division, and each variable possesses a statistical distribution that factors its model uncertainty. In order to emphasise the uncertainties, the distribution can be based on the und, underlying properties of the random variable. The probability distribution is based on the underlying properties of the random variable. In this study, the statistical properties of the random variables are taken from the most practical recommendations of JCSS [18], Ellingwood [25], Fisher & Galambos [26], Galambos & Ravindra [27], Kennedy & Gad Aly [28], whilst the section properties are taken from Melcher et al. [29], Holicky & Sykora [30]. In addition, the past research provides the existing steel data, including 1923-A3, 1936-A36, 1955-A36, and 1963-A36 steel products with strengths of 124, 138, 158, and 158 MPa [25]. The upper range for yield strength can be determined by 0.95(fy − 4 *ksi*) or 0.95(fy − 28 MPa) [25], and specific variables related to the TA-SP connection are outlined in the following Table 1.

Table 1. Statistical variables and probability distributions.

Variables	Symbol	Distribution	E [ ]	Cov
Section model	Zx	Normal	1.00	0.05
Thickness	t	Normal	0.964	0.039 0.025
Yield stress	f_y	Log-normal	1.05	0.110
Elastic Modulus	E_M	Log-normal	1.00	0.060
Fillet weld	w_n	Log-normal	0.88	0.150
height & width	$h\&w$	Normal	1.00	0.002

The average tension strength for the fillet weld section is about 1.05, with a coefficient of variation of 0.04 [26]. The shear strength ratio to electrode tensile strength is about 0.84 with a coefficient variation of 0.1, while the shear weld strength ratio is 0.88 with a coefficient of variation of 0.11. However, if the weld fabrication is involved, a coefficient of variation of 0.15 is recommended [26].

2.3. Ultimate Moment Capacity of the TA-SP Connection

The clockwise rotational mechanism of the existing connection operates as a locked series system, transmitting a tensile force into individual elements. The strengths of the connection's weakest elements can influence failure. For example, Figure 4(a) schematically illustrates the existing connection-locked chain series system, and the weakest element among the individual elements indicates the failure in a series system.
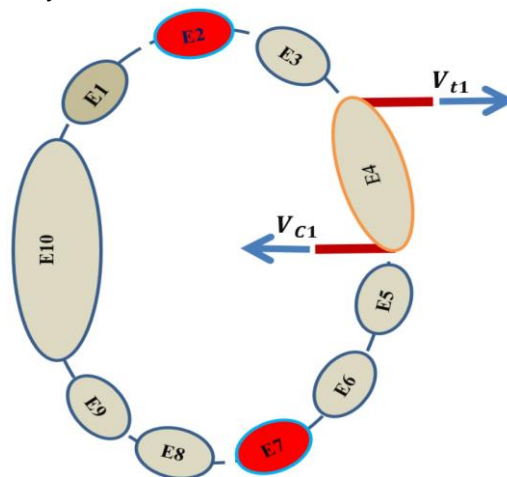

Figure 4. a): Locked-chained elements of the TA-SP connection in a series system.

Unlike elements, (E3) and (E9) operate subsystems in parallel, requiring separate assessments. In simpler terms, assessing the parallel systems is a complicated and exceptional process, as schematically illustrated in Figure 4(b). However, these subsystems are limited to small activities and occur in sequence, even though they are not necessarily as they are related to stochastic variables.
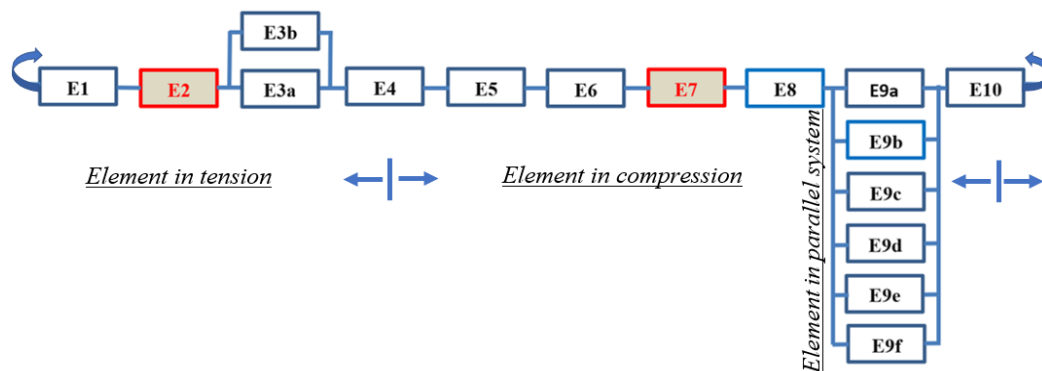

Figure 4. b): Clockwise rotational failure mechanism in series system configurations.

The system's failure is contingent upon the strength of its weakest element. In this context, the Drucker yield criterion [31] helps as a primary tool for evaluating the ultimate tensile shear force exerted on the locked chain-series system. Notably, the prying force exerted by fasteners (E1) and (E3) is pivotal, resulting in tension forces (V_{t1}) due to contact effects, thereby altering the geometrical and material strength changes of the connected element (E2). In this context, failure mechanisms play a crucial role in defining the limit state function for each element within the system. Subsequently,

Tresca's yield criterion [32] arises as pivotal in determining the limit state condition for the weakest element (E2), indicating the most vulnerable link, in the system:

$$g(X)_{E2} \approx \frac{f_y b t_t^2}{4} \geq \varphi_n \, g_1 \frac{V_{t1}}{2}. \tag{6}$$

Where φ_n is a proportional load factor (PLF), g_1 is the gauge length V_{t1} is applied tensile force. In addition, the Australian Standard gives the limit state function of the weld section [33].

$$(X)_{E7} \approx V_{Res}^* \geq \emptyset V_W, \tag{7}$$

Where: $V_{Res}^* \approx \sqrt{(V_X^*)^2 + (V_Y^*)^2 + (V_Z^*)^2}$, $\quad V_X^* \approx 0, \quad V_Y^* \approx \frac{f_y}{2L_w}, \quad V_Z^* \approx \frac{V_{c1}}{2b'} \pm \frac{M_X^* \pm \frac{T_d}{2}}{b' \frac{T_d}{2}}$

Thus, $M_X^* \approx \varphi_n(V_{t1}\, d_3 - V_{c1}\, d_4)$, and $\emptyset V_W \approx 0.6 f_{uw}(T_d + 1.5mm)$ in K. N./m

Where V_{c1} is a compressive force, M_X^* is the moment at the centre of rotation, T_d is a weld throat depth and f_{uw}, denoted by the ultimate strength of the weld section. Among other things, the general procedure is linked with the moment–rotation relationship behaviour and the connection curve parameters can be discussed using the curve-fitting approaches. In this context, the preceding equation for the ultimate moment capacity of the existing TA-SP connection is given by:

$$M_u \approx \varphi_n \frac{g_1 V_{t1}}{2} - \varphi_n(V_{t1}\, d_3 - V_{c1}\, d_4) + \frac{0.6 b'(T_d)^2}{4} f_y, \tag{8}$$

It is also essential to note that the moment-rotation relationships can be effectively expressed in a self-contained format, enabling easy reference to Equation 8. The parameters, such as initial stiffness, ultimate moment, and rotational capacity, can be cross-referenced with the author's previous work to avoid duplication (see Appendix A).

3. Analysing the Weakest Element Failure Mechanisms in the System

The study extends an investigation initiative that evaluated the numerical and analytical performance of the existing connection elements. A prototype of the connection was developed, and the gauge distance was assessed by adjusting the thickness of the vertical leg and stretching (gauge length) limits, thus migrating inelastic demands from the beam-column interface. For this purpose, Figure 5 illustrates the prototype of the existing TA-SP connection and its geometrical parameters are outlined in Table 2 for meticulous analysis of the connection responses, mainly focusing on measuring the failure mechanisms and the load-carrying capacities of the weakest elements in the system.
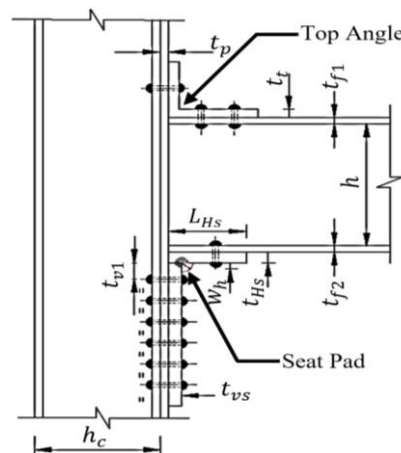

Figure 5. 1920s to 1960s classes TA-SP connection considered in this study prototype.

Table 2. Geometrical parameter of the existing connection.

Beam	W14 × 38
Column	W12 × 96
Top Angle	152.4 × 101.6 × 12.7mm
Seat Pad	100(H) × 19.1 + 350(V) × 22.23mm
Rivet-∅	22.0mm
Accessory plate	10.0mm

The conventional method for assessing the weakest element involves the failure and safe state. To better understand, Figure 6 illustrates the failure mechanism of the weakest elements during the full range of the beam rotation's hysteretic behaviour.
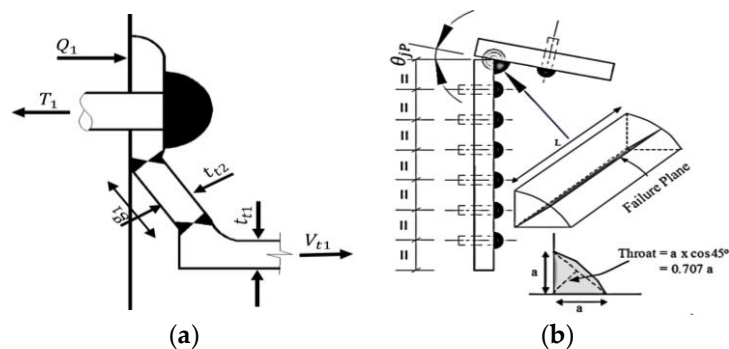

(**a**)   (**b**)

Figure 6. Failure mechanism of the weakest link elements: (**a**) represents the Top angle (E2) failure mechanism under tensile force and (**b**) describes the Seat-Pad weld (E7) failure mechanism behaviours under compressive force.

At gauge, distance (g_1), in both scenarios exhibits identical effects, ensuring equal pre-yield stiffness under unformed transferred force. However, while both elements initially demonstrate comparable pre-yielding behaviour at similar gauge distances, their responses diverge post-yielding. This leads to decreased capacities and heightened sensitivity to overall connection stability, as illustrated in   Figures 7(a) and 7(b)   for their failure and safe states, respectively. Their analyses entail incrementally varying the Proportional Load Factor (PLF) from 0.0 to 1.0 between the ultimate and plastic moment capacity connection responses, as elaborated in Appendix A. Their conditions are initially expressed by Equations 6 and 7 and involve a linear analysis focusing on the connection responses represented in the failure mode. It also elucidates the distinctive failure mechanisms of these weakest elements, comparing the ultimate beam rotation yields when assigned to 119.2 kN ultimate tensile force.
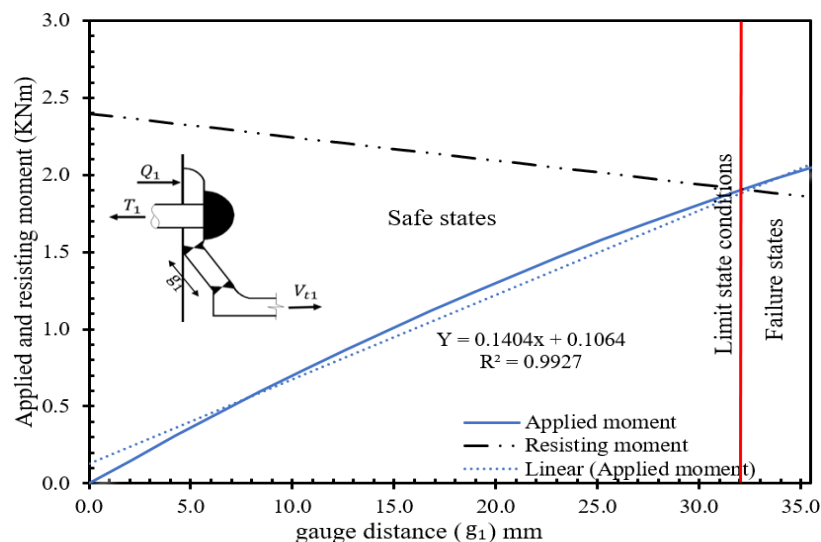
Figure 7. a): Applied and resisting moment Vs to the gauge length-Element (E2).
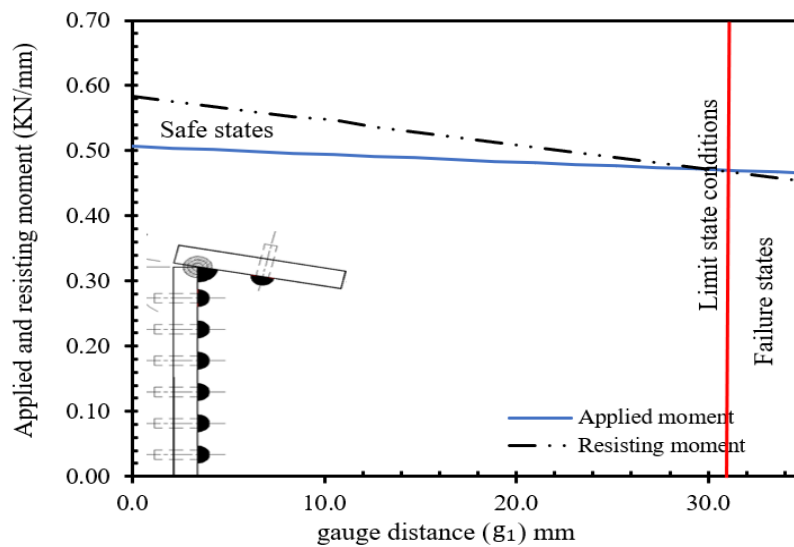

Figure 7. b): Applied and resisting moment Vs to the gauge length-Element (E7).

To further validate these findings, the subsequent section delves into how the weakest elements influence the nonlinear moment-rotation relationship under the beam's clockwise rotational failure mechanism, providing additional justification for the proposed analysis.

4.0. Modelling Finite Element Method

Three-dimensional nonlinear F.E. models were developed in ABOUCS [19] commercial software for the existing TA-SP connection. The steel material with $fy \approx 210$ MPa and $fu \approx 435$ MPa yield strength is used for beams and columns, and a 0.2% post-yield stiffness ratio is used in both cases. The connection between the top angles, seat pad, beam, and column is modelled as a system of nonlinear elements with distributed plasticity, and the load will transmute from the beam to the column via riveted top angles and seat pad connection. This arrangement is depicted in Figure 8 using a 3D finite element model.

Figure 8. The existing TA-SP connection 3D model.
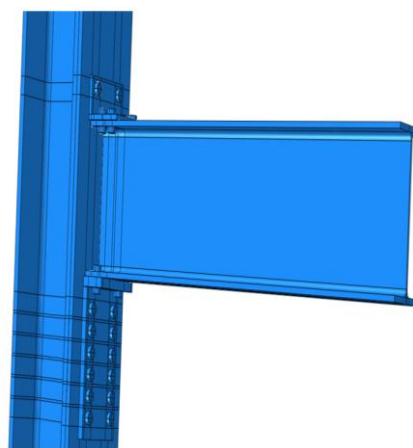
The number of independent contact interfaces was considered for the suitable interaction between the connected portions. Contact-friction interfaces are used to simulate the contact between each element and the surrounding parts. Figure 9 illustrates the advanced modelling implemented in the von Mises yield criterion [34], which services the simplified model strategy.
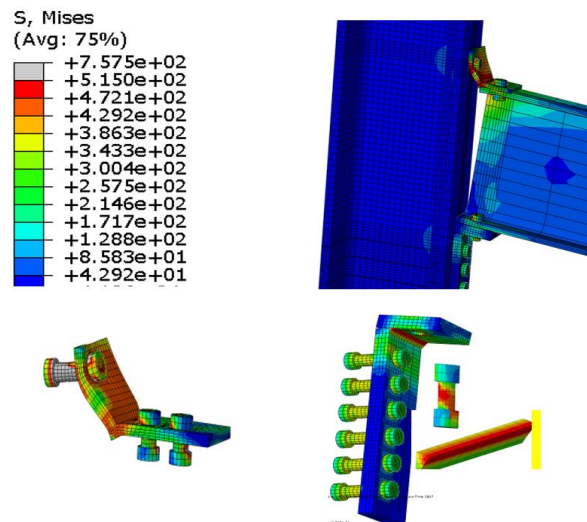
Figure 9. The von Mises criterion under the ultimate load of the TA-SP connection clockwise rotational failure mechanism behaviours.

The fastener pretension was applied for a thermal gradient on the fastener yield. Since there is no information about the amount of fastener pretension in the earlier study, the design values of the pretension force described by ANSI/AISC 360-10 [35] were applied. At the initial loading stage, about 178 kN pretension force was used for a 22.3 mm diameter rivet fastener. Each element was modelled based on a plastic-borne approach, and zero nonlinear rotations were placed to simulate the formation of hinges in the weakest elements. These effects can also translate to the moment-rotation relationship curve expressing the curve parameters mode.

4.1. Validation

Indeed, to facilitate the practical application of the nonlinear F.E. mothed process, the moment-rotation curve that includes essential parameters like initial stiffness (Rki), ultimate moment resistance (Mu), and shape parameters (n) at different curve levels employed, enabling a more profound consideration of the weakest element's effect as depicted in Figure 10. This highlights the critical parameter mode of the existing TA-SP connection, offering valuable insights into the connection behaviours.

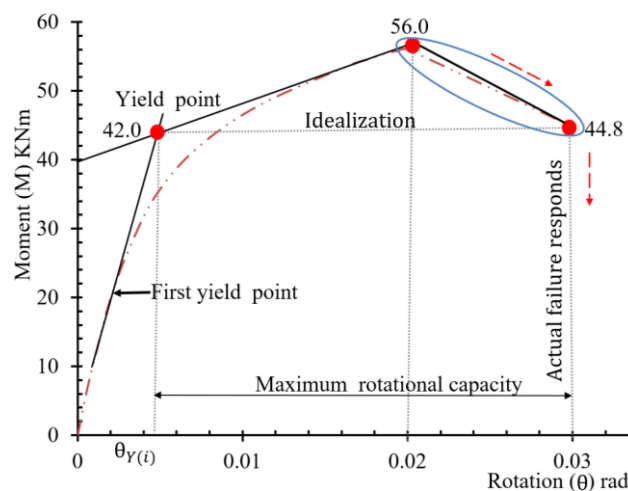
Figure 10. Moment-rotation relationship curve describing the TA-SP connection parameters.

Indeed, the analysis reveals an elastic-to-plastic transition examined at increments of 0.01 rotation. As per ANSI/AISC 360-10 guidelines [35], the rotational limit for ultimate resistance stands at 0.02 radians. In addition, the plastic resistance rotation for stiffness degradation during a complete

cycle is about 0.03 radians, as evidenced in the moment-rotation relationship curve of this study. While comparing the predicted results with those of the F.E. model, the F.E. method yielded slightly superior results than the analytically predicted value (see Appendix A). Nonetheless, both methods demonstrated relatively close results and accurately captured the behaviour of the TA-SP connection parameters.

5.0. Structural Reliability Methods

This study introduces structural reliability for evaluating the TA-SP connection system. It discusses commonly used techniques, like FORM [20] and SORM [21], to simplify calculations and determine the reliability index. The Monte Carlo Simulation (MCS) [22] was introduced to compare the results' accuracy. Meanwhile, advanced computational tools like MATCAD [36] and spreadsheets were employed to streamline simulations (see Appendix B).

5.1. First-Order Reliability Method FORM

The First Order Reliability Method aims to represent uncorrelated random variables in a linear limit state function utilising the first and second moments [37]. The method includes the First-Order Second-Moment (FOSM) and the Advanced First-Order Second-Moment (AFOSM) approach. The FOSM method ignores information about the distribution of random variables. Conversely, the distribution of random variables is aptly utilised in AFOSM.

5.1.1. Estimating the Probability of Failure Using FOSM

The clockwise rotational mechanism of the existing connection represents an optimal scenario for plastic failure, delineating the minimum reliability of its weakest elements. The connection system is deterministic and distributes the tensile force equally among elements despite variations in strength and size. The FOSM approximation is ideal but encounters limitations due to the first-order Taylor expansion for managing the nonlinear limit state functions. Thus, the failure probability of the weakest element can be estimated by substituting Equation 1 and 4 into Equation 9.

$$P_{fi} \approx F_V(V_t) \approx \Phi(-\beta_2)_{E2}, \quad for \quad E7 \approx \Phi(-\beta_7)_{E7}, \tag{9}$$

Consequently, it can be simplified by including the Proportional Load Factor:

$$P_f \approx \Phi\left(\frac{\varphi_n(R_i) - \varphi_n(S_i)}{\sqrt{\sigma_{Ri}^2 + \sigma_{Si}^2}}\right)_{E2} \& \quad \Phi\left(\frac{\varphi_n(R_i) - \varphi_n(S_i)}{\sqrt{\sigma_{Ri}^2 + \sigma_{Si}^2}}\right)_{E7}, \tag{10}$$

The resistance and the load will be modelled as independent Gaussian random variables with N(μRi, σRi) and N(μSi, σSi), respectively. Where *Si* is the mean value of the applied moment at the *i-th* element and, relatively, *Ri* is the mean value of the plastic moment capacity of the *i-th* element, φ_n, is Proportional Load Factor (PLF) ranging from 0.0 to 1.0, and σ_{Ri} & σ_{Si}, is the standard devotion for *the i-th* element. The equation for calculating the reliability index of the TA-SP connection can be expressed by the inverse cumulative distribution of the standard normal function [20,38]:

$$\beta_{FORM} \approx \Phi^{-1}(P_f), \tag{11}$$

5.1.2. Estimating the Probability of Failure Using AFOSM

Advanced First-Order Second Moment is the transition of the reduced variable in the standardised coordinated system [37], and thus, the reduced random variable be expressed by:

$$X_i' \approx \frac{X_i - \mu_{xi}}{\sigma_{xi}}, \tag{12}$$

Where *i* is designated by $E_1, E_2 \dots \dots E_{10}$, of the limit state function of the component as referred to in Equation 3 and can be rewritten as $g(X_1' X_2' \dots\dots X_n') \approx 0$. This represents the minimum vector distance point from the origin of x*and simplifies the random variables of $(X_1 X_2 \dots\dots X_n)$ at the design

point. However, for a more refined analysis of consistent coordination, the Hasofer-Lind reliability index [39] can be used to determine the minimum vector distance point from the limit state surface:

$$\beta_{HL} \approx \sqrt{(x'^*)^T (x'^*)}, \tag{13}$$

It also represents the minimum random variables of the load-carrying capacity (R_i'), and the applied moment (S_i'). Both variables are independent and expressed by Gaussian random variables $N(\mu_{ri}, \ \sigma_{X_{ri}})$ and $N(\mu_{mi}, \ \sigma_{X_{mi}})$:

$$R_i' \approx \varphi_n \frac{R_i - \mu_{ri}}{\sigma_{X_{ri}}}, \qquad S_i' \approx \varphi_n \frac{S_i - \mu_{mi}}{\sigma_{X_{mi}}}, \tag{14}$$

From this perspective, the limit state function can be driven by:

$$Z_i \approx \sigma_{X_{ri}} R_i' - \sigma_{X_{mi}} S_i' + \mu_{ri} - \mu_{mi} \approx 0, \tag{15}$$

Where Z_i, is a Gaussian distribution comprising the chain rules. As such, the partial derivative of the performance function at the design point of the origin is given by:

$$\left.\frac{\partial_g}{\partial_{fy}}\right|_{\partial X_i^*} \left(\sigma_{fy}\right)_i; \qquad \left.\frac{\partial_g}{\partial_{zp}}\right|_{\partial X_i^*} \left(\sigma_{z_{pl}}\right)_i, \tag{16}$$

Then, the reduced design point ($n-1$) of the variable is expressed by:

$$f_{y1}^* \approx \left(\mu_{fy} + \sigma_{fy}\beta\alpha_{fy}\right)_i \qquad Z^*{}_1 = (\mu_z + \sigma_z\beta\alpha_z)_i, \tag{17}$$

Where α_n is a direction cosine at the minimum distance point of x_i^*, that could be articulated by the following equation [40]:

$$\alpha_{fy} \approx \left(\frac{-\sigma_{fy} f_y^*}{\sqrt{\left(\sigma_{fy} fy^*\right)^2 + (\sigma_z Z^*)^2}}\right)_i \quad \alpha_Z \approx \left(\frac{-\sigma_z f_y^*}{\sqrt{\left(\sigma_{fy} Z^*\right)^2 + (\sigma_z fy^*)^2}}\right)_i, \tag{18}$$

Hence, the normalised value of the design point at the origin space is given by:

$$x^*{}_i \approx (\beta^2 \alpha_Z \alpha_{fy} + \beta\alpha_Z + \mu_{fy}\mu_z)_i, \tag{19}$$

Accordingly, Figure 11 illustrates the uncorrelated minimum distance point at the limit state surface for elements E2 and E7.
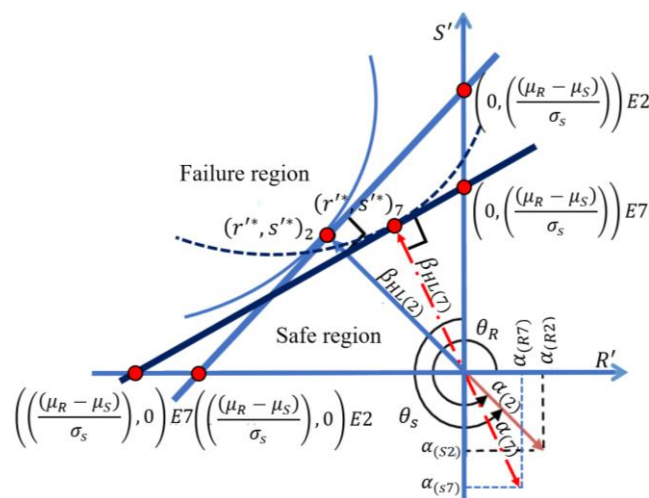

Figure 11. Uncorrelated coordinate of the minimum distance from the origin.

Where r'^* and s'^*, denote the design points at the limit state surface, reflecting the reduced reliability index. Accordingly, Table 3 elucidates this convergence, observed at the third iteration cycle, indicating their corresponding failure probabilities.

Table 3. Summary of the iterative cycle**.**

Iteration cycle	Element (E2)		Element (E7)	
No	(β_{HL})	(P_f)	(β_{HL})	(P_f)
1	-3.098	9.73E-04	−3.199	6.89E-04
2	-3.080	4.26E-03	−3.198	6.93E-04
3	-3.080	1.04E-03	−3.198	6.93E-04

5.2. Estimating the Probability of Failure Using SORM

The Second-Order Reliability Method (SORM) is a technique used for reliability analysis that considers the second-order effects. It provides a more accurate estimation of the reliability index by considering the nonlinearity of the limit state function and the non-normal distribution of input variables at the limit state surface [21]. SORM is a robust method that quickly delivers reliable results using the First-Order Reliability Method (FORM). The method involves the Rosenblatt transformation [41], which converts random variables X_i, to a non-normal distribution in the U space. The conversion of the random variables X_i to standard variables is given by:

$$Y_i \approx \frac{X_i - \mu_{Xi}^e}{\sigma_{Xi}^e},$$ (20)

The mean (μ_{Xi}^e) and standard deviation (σ_{Xi}^e) of X_i, for the minimum distance of a design point (x_i^*) are crucial parameters. Similar methodologies are applied to estimate the equivalent parameters for log-normal X_i. The failure probability can be computed using the probabilistic model of $g(X_i)$, representing the direction cosine at the minimum distance design point [37]. This approach is applied to the TA-SP connection elements, as depicted in Figure 12, with its background briefly discussed in a prior study [42].
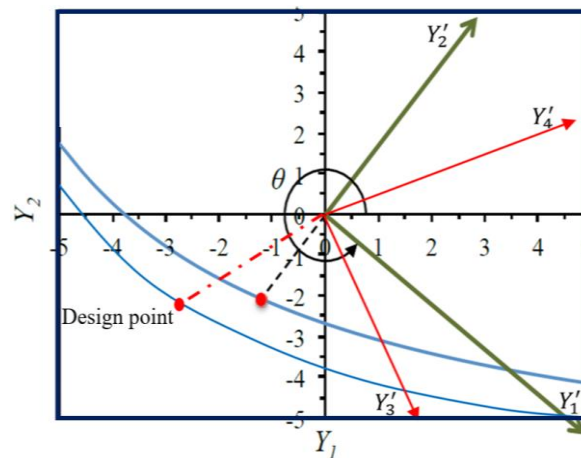
Figure 12. Uncorrelated variables rotation at the axis of the reduced space.

The Rosenblatt transformation is a differential operator wherein the eigenvector function scale is definite by (*n* x 1) matrix with the differential equations. The relationship between the eigenvector function and the decomposed diagonalised matrix encompasses the rotational coordination (θ). by emphasising its geometrical descriptions. Such perspective has a diagonalised matrix that the following equation can formulate:

$$B_i \approx \begin{bmatrix} Cos\theta & \cdots & Sin\theta \\ \vdots & \ddots & \vdots \\ -Sin\theta & \cdots & Cos\theta \end{bmatrix}_i,$$ (21)

Where θ = 270º + tan–1(y_2^*/y_1^*), and y_n^* is the x_n^*, transforms the random variable to the reduced distance. Consequently, for determining the second derivative performance function of the chain rule differentiation. Such expression in matrix form is given by:

$$D_i \approx \begin{vmatrix} \dfrac{\partial_g^2}{\partial Y_1^2} & \dfrac{\partial_g^2}{\partial Y_1 Y_2} \\ \dfrac{\partial_g^2}{\partial Y_1 Y_2} & \dfrac{\partial_g^2}{\partial Y_2^2} \end{vmatrix}_i = \begin{vmatrix} 0 & x_2^* \sigma_{x1} \\ x_1^* \sigma_{x2} & 0 \end{vmatrix}_i , \tag{22}$$

Hence, the second derivative of the limit state function at the design point is given by:

$$A_i \approx \left| \begin{matrix} \left[cos\theta + \left(\dfrac{\partial_g^2}{\partial Y_1^2} \right) + \dfrac{0.8 cos\theta}{|\nabla G(y_n^*)|} \right] & \left[sin\theta + \left(\dfrac{\partial_g^2}{\partial Y_1 Y_2} \right) + \dfrac{0.8 sin\theta}{|\nabla G(y_n^*)|} \right] \\ \left[-sin\theta + \left(\dfrac{\partial_g^2}{\partial Y_1 Y_2} \right) + \dfrac{0.8 sin\theta}{|\nabla G(y_n^*)|} \right] & \left[cos\theta + \left(\dfrac{\partial_g^2}{\partial Y_2^2} \right) + \dfrac{0.8 cos\theta}{|\nabla G(y_n^*)|} \right] \end{matrix} \right|_i , \tag{23}$$

Where i is an individual connection element of $(E_1, E_2 \dots E_{10})$ and thus, the last row and last column are computed for the eigenvalues of the matrix A_i. Intrinsically, the system failure probability approximation is given by taking the eigenvalue (v_i) of the matrix A_i, into account [21]:

$$P_{fE2} \approx \left[\Phi(-\beta_2) \prod_{i=1}^{n-1} (1 + \beta_2 v_2)^{-1/2} \right]_{E_2} , \; P_{fE7} \approx \left[\Phi(-\beta_7) \prod_{i=1}^{n-1} (1 + \beta_7 v_7)^{-1/2} \right]_{E_7} , \tag{24}$$

Where β_2 and β_7 are first-order reliability indexes [20] representing elements E2 and E7. Accordingly, Equation 24 can be transformed into the inverse standard normal distribution function, expressing the weakest elements' reliability index.

6.0. Results in Percental Error

In order to compare FORM and SORM precision, ten thousand simulations were performed using the Monte Carlo Simulation (MCS) [22], measuring the number of performance functions g(x). Furthermore, the system reliability-based analysis, where the performance function is more efficient in determining the probabilities of failure. As for efficiency, recent literature highlights the percentile error as a measure of efficiency, comparing the probability of failure. This generally involves a set of numbers that indicate the fractional difference in calculating the probabilistic model [43]. Thus, control of the percental error is given by:

$$Error\, \% \approx \left(\frac{P_f - P_{f\,MCS}}{P_{f\,MCS}} \right) \times 100 , \tag{25}$$

In this respect, the MCS provides a reference for comparison, and Table 4 presents the calculated probabilities of failure and the percentile error and plots the corresponding failure mechanism of the existing TA-SP connection in Figures 13 and 14.
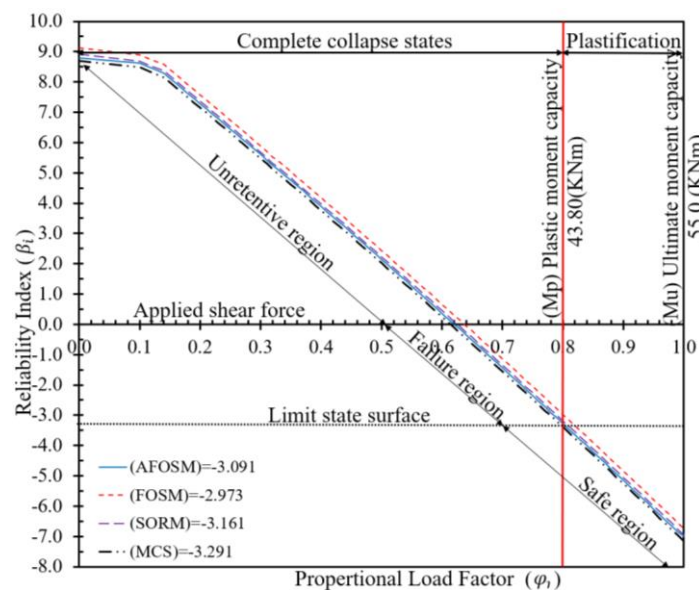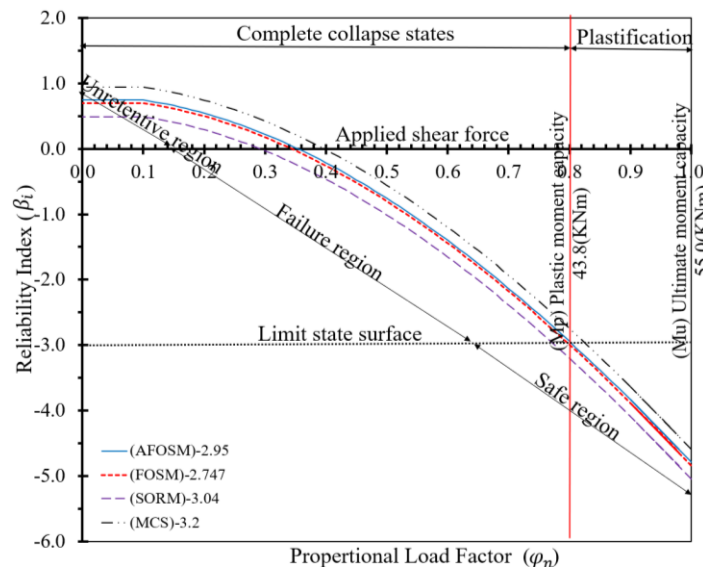
Figure 13. Variation of the reliability index vs. proportional load factor - Element (E2).

Figure 14. Variation of the reliability index vs. proportional load factor - Element (E7).

Table 4. Failure probability and percentile Error.

Types	Top angle (E2)			Weld (E7)		
	β	P_f	Error	β	P_f	Error
AFOSM	−3.09	9.99E-04	100.1%	−2.92	1.74E-03	113.1%
FOSM	−2.97	1.48E-03	195.6%	−2.75	2.96E-03	262.1%
SORM	−3.16	7.86E-04	57.4%	−3.05	1.16E-04	42.4%
MCS	−3.29	4.99E-04		−3.15	8.16E-04	

While each method meets stable conditions, the AFOSM and FOSM overestimate the probability of failure, exhibiting lower efficiency than SORM in percentile errors. Specifically, SORM yields about 27.1% and 49.7% higher than the AFOSM and 87.7% and 154.33% higher than the FOSM. This discrepancy is expected as SORM accounts for both first and second-order effects, capturing the curvature of the performance function.

Similarly, MCS yields approximately 100.1% and 113.1% higher values than AFOSM and 195.6% and 262.1% higher than FOSM. However, it captures 80% and 65.7% of the overall percentile errors. Comparing SORM with MCS is a crucial part of the study; the MCS is approximately 57.4% higher in E2 and 45.99% higher in E7. Despite these differences, they are almost close in their order of magnitude and are not very significant.

7.0. System Reliability Analysis of the Existing TA-SP Connection

Over the past four decades, extensive research has focused on evaluating the reliability of individual structural members to inform design codes. However, upon comparing the reliability of single members to that of entire systems, it becomes apparent that the system consistently exhibits higher reliability due to the advantageous load distribution effect. Various failure modes are examined in assessing the existing TA-SP connection, treating each element model as a parallel system. This approach allows the overall system to be conceptualised as a series of parallel systems [44]. The analysis employs rigorous methods to forecast the reliability index, assigning each element its potential failure mode within the *i-th* element of the system. Ultimately, the weakest link in the system determines the connection's overall failure, as illustrated in Figure 15. Such probability of system failure can be expressed by rearranging Equation 5.
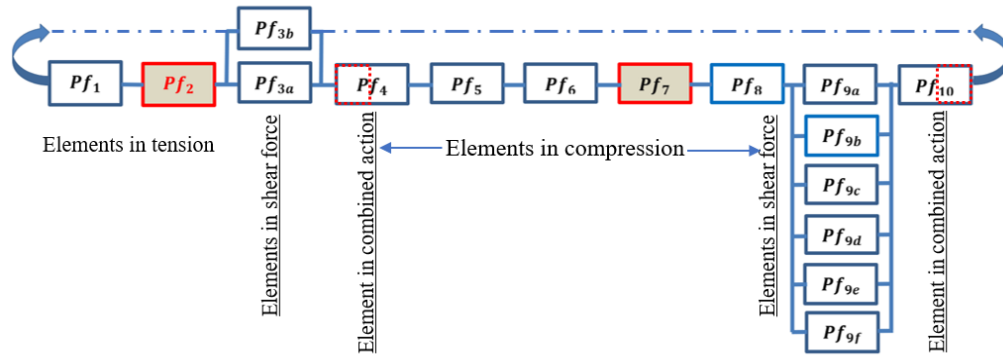
Figure 15. Clockwise Rotational Failure Mechanism in the Chain Series System of the Existing TA-SP Connection.

$$(P_f)_S \approx \sum_{i=1}^{n}(P_f)_1 + \cdots (P_f)_2 \ldots + (P_f)_7 \ldots + (P_f)_n \,, \tag{26}$$

Where $i = 2$ and $i = 7$ elements enclose the relationships among the union of the weakest link events. A typical chain series system describing the clockwise rotational mechanism under tension, compression, and combined actions is illustrated in Figure 15.

Likewise, the performance function of the series system can be transformed into the inverse standard normal distribution function. This allows for determining the system reliability index concerning the clockwise rotational mechanism of the TA-SP connection, emphasising the influence of the weakest elements in the chain series system.

$$\beta_S \approx -\Phi^{-1}\left[(P_f)_2 + (P_f)_7\right], \tag{27}$$

A comparison of the system failure probabilities and the percentile errors is summarised in the following Table 5.

Table 5. Summary of the Proposed Methods and Percentile Errors.

Type	P_{fS}	β_S	Error (%)
AFOSM	2.74E-03	−2.78	108.2
FOSM	4.43E-03	−2.62	236.8
SORM	1.95E-03	−2.89	48.1
MCS	1.12E-03	−3.03	

8.0. Target Reliability Index Considerations

The reliability-based approach ensures that structures meet a certain level of reliability, exceeding desired target levels through operational design procedures. Establishing standardised procedures for existing steel members, equivalent to new ones, presents challenges but offers the benefits of a reliable framework with built-in margins. Various works explore appropriate target reliability levels, as seen in ISO 13822 [16], ISO 2394 [17], and JCSS [18], where the consequence of failure determines the target reliability index. Progress in standardisation builds upon a substantial foundation of literature and research, including influential papers by Allen [45] and Ellingwood [25].

Nevertheless, recent investigations such as Holicky and Sykora [30], Vrouwenvelder and Vrouwenvelder [46], Tanner et al. [47], Steenbergen et al. [48], Sýkora et al. [49] have significantly contributed to the standards. Their collective work is crucial in shaping and improving the standards and guidelines within the practice or field.

ISO 2394 [17] states that the requirements for assessing existing structures are the same as those for designing a new structure. However, a lower target reliability index may be justified for existing structures based on economic, social, and sustainable factors (ISO 13822, Annex F [50]). For lower

failure consequences, the target reliability index is 2.3. Moderate failure consequences range from 3.1 to 3.8, while higher failure consequences require a target reliability index of 4.3 [17].

FEMA performance assessment guidelines capture a more elaborate literature review [51] and offer detailed insights, suggesting a failure probability of less than 5% to avoid severe damage, signifying a hazard that encounters a 99.9% failure probability. Melcher et al. [29] repeated a 5% probability of failure, and a 1.75 reliability index is recommended for the existing structural member subjected to earthquake shaking. The most relevant information is effectively embedded in the LRFD specification. This could serve as background input, and the target reliability index ranges from 2.5 to 3.0 [2]. Similarly, JCSS [18] provides the structural performance requirements with single and multiple failure probabilities. Additionally, Fischer et al. propose acceptance criteria of 2.7 to 3.0 for ductile failure members and 2.8 to 3.4 for brittle failure, considering life safety consequences [52].

The comparison of the present study outlined in Table 5 highlighted the significance of adhering to the proper reliability index level. It highlights the alignment with the lower reliability index implied by the acceptance criteria. The consecutive steps of the lower target reliability index range from 2.3 to 2.5, corresponding to the consequences of failure, operational lifetime, and the cost of safety measures [2,17,18]. However, these guidelines indicate an acceptable reliability index (βa) lower than the design values for the single-element reliability index (see Table 5), emphasising the relative contributions of plastic and ductile failure mechanisms.

9.0. Conclusion

The article introduces a vital breakthrough in research and structural engineering practice. It proposes new techniques for evaluating the system reliability of existing TA-SP connections, which show significant advances. These methods align with the limit state approaches for designing new semi-rigid connection models. Providing a comparative study of the TA-SP connection behaviours to the revised equations proposed by Kishi and Chen [5] also demonstrated the efficacy of the initial stiffness, ultimate moment capacity, and stiffness degradation of the existing TA-SP connection.

The study extended its scope for assessing the nonlinear finite element (F.E.) analysis of the moment-rotation relationship behaviours, implying the connection performance and consistency of the three-parameter power model.

Further to the finite element analysis, a new closed-chain series system method has been introduced, incorporating a rule-based process to account for uncertainties in material properties, geometric properties, and models to ensure safety. This new process involves evaluating the linear approximation of the limit state function, followed by second-order second-moment approximations to obtain the nonlinear limit state at the performance surface [21]. This involves delving into the failure probability of the weakest link elements in the connection system, employing advanced assessment methods that yield more refined verification and include rigorous reliability and system reliability-based analysis. A comparison between the First Order Reliability Method (FORM) and the Second Order Reliability Method (SORM) was conducted, revealing their disparities in the approximations. The percentile error was used to measure their differences based on 10,000 sample tests of the Monte Carlo Simulation reference (MCS) [22], confirming compliance and adhering to ISO 13822 [16], ISO 2394 [17], and JCSS [18], standards was paramount to meet the target reliability index.

In conclusion, the study lays the groundwork for integrating technical specifications into the next version of the semi-rigid connection assessment framework. By leveraging harmonised relationships among semi-rigid connection counterparts, the proposed methods offer an opportunity to introduce new assessment methods into the standard that present two distinct perspectives: one proposing an alternative methodology for advanced assessment analysis verified against AN-SI/AISC 360-10 [35], Eurocode 3 Part 1-8 [3], and the other one is introduced in a more operational analysis to standardise the existing connection system reliability index. Both perspectives yield significant results, offering practical applications for experts, specialists, engineers, and researchers engaged in high-reliability verification of aging buildings. Therefore, the methodologies introduced

are custom-made to meet the demands of professionals seeking meticulous assessment frameworks in the field.

Notation

The following symbols are used in this paper:

$\emptyset$ = 0.6 or 0.8 fillet weld category

ϕ^{-1} = inverse cumulative distribution of the standard function

$\cup$ =union operator in set

$\cap$ = set intersection operator between two sets

φ_n = proportional load factor (PLF)

σ = standard devotion

μ = mean value

v = eigenvalue function scale

β = reliability index

α_n = direction cosine at the minimum distance point

a = Weld throat length and height

A_i = second derivative limit state function at the design point

b = top angle width

b' = weld section width

B_i = decomposed diagonalised matrix

d_3 = distance at the centre of rotation

d_4 = distance at the centre of rotation

D_i = second derivative performance function

E = event failure in an i-th mode

En = failure state of the weakest link element

E_M = Elastic Modulus

Fi = shear force function in i-th element

$f_x(x)$ = probability density function of stochastic variables

$F_{Ri}(r)$ = the cumulative distribution function of the strength

f_y = yield stress

fu = yield strength

f_{uw} = yield stress of the weld section

g_1 = gauge length

$g(X)$ = limit state function,

h = height

i   = the failure event of the i-th element, (i = 1, 2, … n)

k_r = reduction factor 1.0 for all connection

M_X^* = moment at the centre of the weald section

M_u = ultimate moment capacity of the connection

n = shape parameter of the connection

P_f = probability of failure

r'^*= design point at the limit state surface

Ri = mean value of the plastic moment capacity

$R'i$ = reduced resistance element random variables

Rki = initial stiffness of the TA-SP connection

s'^* = design point at the limit state surface

S_i = mean value of the applied moment for the i-th element

S'i = reduced applied moment random variables

T_d = seat-pad weld throat depth

t_t = top angle thickness

V_{c1} = applied compressive force

V_{t1}= applied tensile force

V_{Res}^* = applied moment to weld section

V_X^* = applied monent to x direction

V_Y^* = applied moment to y direction

V_W = Nominal capacity of fillet weld

V_Z^* = applied moment to z-direction

w   = width

w_n= Fillet weld

x^* = vector distance point from the origin space

X   =   vector of stochastic variables

X_{Fi}, = applied force to the i-th element

X_i'= reduced random variable for i-th element

X_i = tensile force distribution among the elements

X_{Ri} = resistance element for i-th element

Y_i= transformation of a random variable to standard variables

Z_i = Gaussian distribution comprising the chain rules

Zx = Modulus of section

Z_{ew} = Modulus of weld section-

References

1. M. Hardy Cross, "Analysis of continuous framing by distributing fixed moments," *AISC, American Society of Civil Engineering*, 1930, Vol. 96 (1).
2. American Institute of Steel Construction AISC "Manual of steel construction," load and resistance factor design-LRFD, *Second ed,* AISC, 1994, Chicago IL, U.S.
3. EN 1993 Eurocode 3: "Design of steel structures part 1– 1: general building rules," 2005.
4. R.M. Richard. & B.J. Abbott, "Versatile elastic-plastic stress and strain formula",–*Journal Engineering Mechanical Division*, (*ASCE*), 1975, Vol. 101, no. 4, pp. 511515.
5. N. Kishi, & W. F. Chen, "Moment-rotation relations of semi-rigid connections with angles", *Journal of Structure Engineering,* (*ASCE*), 1987, Vol. 116, no. 7, pp. 1813-1834.
6. A. Colson, & J.M. Louveau, "Connections Incidence on the Inelastic Behaviour of Steel Structural", Euromech Colloquium, 174, 1983.
7. A. Azizinamini et al., "Cyclic characteristics of bolted semi-rigid steel beam to column connections."PhD thesis.," Dept. Civ. Engrg., Univ. of South Carolina, Columbia, SC., 1985.
8. R. Bjorhovde, A. Colson, & J. Brozzetti, "Classification system for beam-to-column connections," *Journal of Structural Engineering, (AISC),* 1990, Vol. 116, no. 11, pp. 3059-3076.
9. G. Pekcan, J.B. Mander, & S.S. Chen, *Experimental & analytical study of low-cycle fatigue behaviour of semi-rigid top and seat angle connections*, 1995, *NCEER-95-0002.*
10. C. Faella, V. Piluso, and G. Rizzano, "Structural Steel Semi-rigid Connections Theory Design, and Software" *Engineering, Materials Science*, Corpus ID: 107124660, 1999.
11. A. Ahmed, N.Kishi, K.Matsuoka, and M.Komuro, "Nonlinear analysis on prying of top- and seat-angle connections."," *Journal of the. Appled. Mechanics.,* 2001, Vol. 4, no1, pp., 227–236.
12. A. Pirmoz, K. Seyed, A. Mohammadrezapour, E., and D. Saedi, "Moment-rotation behaviour of bolted top-seat angle connections." *Journal of Construction Steel Research, (ELSEVIER),* 2009, Vol. 65 no.4, pp.973– 984.
13. M.S. Smitha and S. Babu "Behaviour of top and seat angle semi-rigid connections," *Journal of the Institution of Engineers (India), -* A, 2014, Vol. 94, no. 3, pp. 153–159.
14. A. Ahmed, "Prediction of the moment–rotation characteristic of top and seat angle bolted connection incorporating prying action." *International Journal of Structural. Engineering,* 2017, Vol. 9, pp. 79–93.
15. C. Diaz, P. Marti, M. Victoria, and M.Querin, "Review on the modelling of joint behaviour in steel frames." *Journal of Construction Steel Research*, (*ELSEVIER*), 2011, Vol. 67 no 5, pp. 741–758.

16. ISO 13822, "Bases for design of structures assessment of existing," ISO TC98/SC2, Geneva, Switzerland, 2010.

17. ISO 2394, "General principles on structure reliability," 2nd ed, ISO, Geneva, Switzerland, 1998.

18. JCSS, "Probabilistic model code," Joint Committee on Structural Safety, Zurich, 2001.

19. ABOUCS, CAE user's manuals. Version 6.14,: Hibbitt Karlsson & Sorensen, RI, USA, 2014.

20. C. Cornell, "A probability-based structural code," *American Concrete Institute Structural Journal*, 1969, Vol. 66 no 12, pp. 974–985.

21. K. Breitung, "Asymptotic Approximations for Multinormal Integrals," *Journal of Engineering Mechanics, (ASCE)*, 1984, Vol. 110, no. 3, pp. 357–366.

22. C. G. Bucher, "Adaptive Sampling an iterative, fast Monte Carlo procedure," *Journal of Structural Safety*, *(ELSEVIER)*, 1988, Vol. 5, no. 2, pp. 119-126.

23. A. Freudenthal, "Safety, reliability and structural design," *Journal of the Structural Division, (ASCE)*, 1961, Vol. 87, no 3, pp. 1–16.

24. W. Weibull, "A statistical theory of the strength of the material," *Proceeding Royal Sweden. Institute Engineering res*, 1939, Vol. 15, pp 1887-1979.

25. B. Ellingwood, "Reliability-based condition assessment and LRFD for existing structures," *Structural Safety, (ELSEVIER)*, 1996, Vol. 18, no. 2 - 3, pp. 67-80.

26. J. Fisher, M. Ravindra, and T. Galambos "Load and resistance factor design criteria for connection," *Journal of the Structural Division, (ASCE)*, 1978, Vol. 104, pp. 1427–1441.

27. T. Galambos, and M. Ravindra, "Properties of steel for use chapter in LRFD," *Journal of the Structural Division,(ASCE)*, 1968, Vol. 104, no. 9, pp. 1459–1468.

28. D.J.L. Kennedy and M. Gad Aly, "Limit states design of steel structures performance factors," *Canadian Journal of Civil Engineering*, 1980, Vol. 7, no 1, pp.45-77,.

29. R. E. Melchers, Structural reliability analyses and prediction, 1st ed, Chichester: New York: Jonh Wiley & Sons Inc, 2017.

30. Sýkora M, Holický M, Marková J, Target reliability levels for assessment of existing structures, culled from M.H. FABER, J. KÖHLER and K. NISHIJIMA, eds. In: Proc. ICASP11, CRC Press/Balkema, pp. 1048-1056, 1-4 August 2011.

31. D.C. Drucker, "The effect of shear on the plastic bending of beams. "*Journal of Applied Mechanics, (ASME)*, 1956, Vol. 23, no. 4, pp. 509–514.

32. H. Tresca, "Sur l'ecoulement des corps solides soumis a de fortes pressions.," *Comptes rendus de l'Académie des Sciences*, 1864Vol. 59,   pp. 754.

33. AS 4100 Australian standard, Steel structures, Australian, 2020.

34. R.E. von Mises, Mechanik der festen Körper im plastisch- deformablen Zustand, Corpus ID: 138864271, *Materials Science,* https://resolver.sub.uni-goettingen.de/purl PPN252457811, 1913.

35. ANSI/AISC 360, Specification for Structural Steel Buildings, American Institute of Steel Construction, Chicago, US, 2010.

36. MATCAD, MATCAD user's manuals, 2014.

37. A. Halder and S. Mahadevan, Probability, Reliability and Statistical Methods in Engineering Design, New York: Jonh Wiley & Sons Inc., 2000.

38. A. Ang, and W. Tang, Probability Concepts in Engineering Planning and Design: Vol. I, Basic Principles, New York: John Wiley & Sons, pp. 409, 1978.

39. A. M. Hasofer and N. C. Lind, "An exact and invariant first-order reliability format," *Journal of Engineering Mechanics*, 1974, Vol. 100, pp. 111–121.

40. R. Rackwitz, B. Flessler, "Structural reliability under combined random load sequences," *Journal of Computers & Structures, (ELSEVIER)*, 1978, Vol. 9, no. 5, pp. 489-494.

41. M. Rosenblatt, "Remarks on a multivariate transformation," *The Annals of Mathematical Statistics*, 1952, Vol. 23, pp. 470-472.

42. E. Bastidas-Arteaga and A.-H. Soubra, Reliability Analysis Methods, in HAL Id: in2p3-01084369, France, HAL Archives Ouvertes ID: in2p3-01084369, University of Nantes, Ge M Laboratory,   UMR CNRS 6183, Nantes, France, 2015.

43. J. Zhang and. X. Du, "A second-order reliability method with first-order efficiency," *The American Society of Mechanical Engineers*, *(ASME)*, 2010, Vol. 132, no. 10, pp 101006 (8 pages).

44. P.Thoft-Christensen, and J.Dalsgård Sørensen "Reliability of structural systems with correlated elements," *Journal of Applied Mathematical Modelling- (ELSEVIER)*, 1982, Vol. 6, pp. 171-178.

45. D. E. Allen, "Limit states criteria for structural evaluation of existing buildings," *Canadian Journal of Civil Engineering*, 1991, Vol. 18, no. 6, pp. 995–1004.

46. T. Vrouwenvelder and N. Scholten," Assessment criteria for existing structures," *Journal of* Structural *Engineering International, (IABSE)*, 2010, Vol. 20, no. 1, pp. 62–65.

47. P. Tanner and C. L. Sarache, "Semi-probabilistic models for the assessment of existing concrete structures," in 11th International Conference on Applications of Statistics and Probability in Civil Engineering, Zurich, Switzerland, 1–4 August 2011.

48. R. Steenbergen, M. Sýkora, D. Diamantidis and M.Holický, "Economic and human safety reliability levels for existing structures," *Structural Concrete journal, fib CEB-FEP*, 2015, Vol.16 no 3. pp. 323-332.

49. ISO, International Organisation for Standardisation/ South African National Standard, 2016a. ISO13822: 2010/SANS 13822:2016. Bases for Design of Structures. Assessment of Existing Structures. Geneva, Switzerland: ISO, 2016.

50. M.Sýkora, D. Diamantidis, M. Holický and K. Jung, "Target reliability for existing structures considering economic and societal aspect," *Journal of Structure and Infrastructure Engineering*, 2016, Vol. 13, no. 1, pp. 181–194.

51. Federal Emergency Management Agency (FEMA), "Interim Guidelines Evaluation, Repair, Modification and Design of Welded Steel Moment Frame," Report (SAC Joint Venture), no. SAC-95-02, Washington, D.C, 1995.

52. K. Fischer, C. Viljoen, J. Köhler, and M. H. Faber, "Optimal and acceptable reliabilities for structural design," *Journal of   Structural Safety, (ELSEVIER)*, 2019 Vol. 76, pp. 149-161.